

Peak-to-Average-Power Reduction for FBMC-based Systems

Sameh Eldessoki*, Johannes Dommel†, Khaled Shawky‡, Lars Thiele†, Robert F.H. Fischer*

*Institute of Communications Engineering, Ulm University, Ulm, Germany

Email: {sameh.eldessoki, robert.fischer}@uni-ulm.de

†Fraunhofer Institute for Telecommunications, Heinrich Hertz Institute, Berlin, Germany

Email: {johannes.dommel, lars.thiele}@hhi.fraunhofer.de

‡Faculty of Information Engineering and Technology, German University in Cairo, Cairo, Egypt

Email: khaled.shawky@guc.edu.eg

I. INTRODUCTION

Filter Bank Multicarrier/Offset Quadrature Amplitude Modulation (FBMC/OQAM) [1] has recently attracted a lot of attention as a potential competitor to the widely adopted cyclic prefix Orthogonal Frequency-Division Multiplexing (CP-OFDM) [2]. Despite of the FBMC/OQAM's superior frequency localization that makes it a potential enabler in the context of opportunistic networks, it still suffers from high peak-to-average power ratio (PAPR) [3]. The idea of PAPR reduction schemes was proposed in the literature of OFDM in order to combat such problem without the loss in power efficiency, an overview of the different schemes is given in [4], [5]. The same idea was then applied FBMC/OQAM [6] using some of the proposed schemes. In this paper, two new PAPR reduction schemes are introduced, the first is called 'two-stage PAPR reduction' set of schemes which is applicable to any multicarrier modulation technique. The second scheme is a modification of a scheme from the literature of OFDM, called 'modified selected mapping (mSLM)', which takes the special structure of the FBMC/OQAM into consideration.

II. SYSTEM MODEL

Filter bank multicarrier (FBMC) is a generalization of the MC modulation concept, where a well-designed prototype filter shapes the modulated signal on each sub-carrier. This filter suppresses the high out-of-band leakage observed in the OFDM's sub-carrier frequency response.

Figure 1 gives the proposed FBMC/OQAM transceiver block diagram based on the implementation proposed in PHYDYAS [3]. The fundamental parts of this block diagram are the OQAM pre-processing and the synthesis filter bank (SFB) at the transmitter side as well as the analysis filter bank (AFB) and the OQAM post-processing at the receiver side.

Using the derivations from [7], the resulting discrete-time baseband FBMC/OQAM signal can be expressed as:

$$s[k] = \sum_{n=-\infty}^{\infty} \sum_{m=0}^{M-1} d_{m,n} \theta_{m,n} \beta_{m,n} p\left[k - n\frac{M}{2}\right] e^{j\frac{2\pi}{M}mk} \quad (1)$$

where k is the high data rate (M/T) sample index at the output of the SFB, m is the sub-carrier index for the

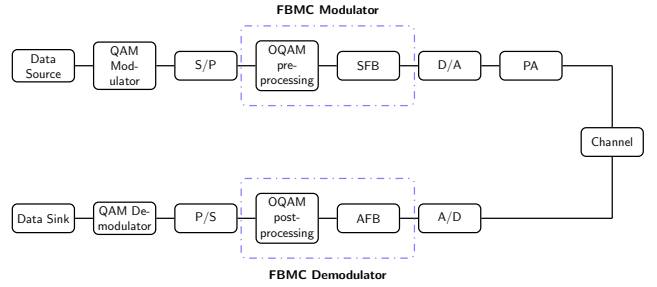


Fig. 1. FBMC/OQAM transceiver chain.

M sub-carriers FBMC/OQAM system, n is the time index at the OQAM symbol's rate ($2/T$), $d_{m,n}$ is the real data sequence before phase mapping. The symbol $\theta_{m,n}$ is defined as $\theta_{m,n} = j^{m+n}$ controlling the phase of the real data sequence at the input of the SFB and $\beta_{m,n}$ is defined as $\beta_{m,n} = (-1)^{mn} \cdot e^{-j\frac{2\pi m}{M}\left(\frac{L_p-1}{2}\right)}$, where L_p is the prototype filter length. $p[k]$ is the impulse response of the prototype filter, where the one proposed in [8] is used. Finally, it should be mentioned that unlike CP-OFDM, FBMC/OQAM has overlapping time symbols as shown in Figure 2, where for this example it is assumed that the number of sub-carriers is $M = 4$, the overlapping factor is $K = 2$, the prototype filter length is $L_{\text{length}} = K \cdot M = 8$, $\text{CP}_{\text{length}} = 1$ and number of QAM symbol vectors is $n_{\text{symbol}} = 2$.

III. PAPR REDUCTION SCHEMES

In this paper five different schemes from the literature of OFDM will be compared, which are clipping [5], tone reservation (TR) [9], active constellation extension (ACE) [10], joint tone reservation and active constellation extension (TRACE) [10] and selected mapping (SLM) [11]. Then the first four schemes are going to be used by our newly presented set of schemes called 'two-stage PAPR reduction'. As evident from the naming the 'two-stage PAPR reduction' set of schemes is formed of one of the iterative clipping based schemes (i.e., TR, ACE, TRACE) as a first stage and then clipping as the second and final stage. This means that it is only a version of the iterative schemes, where after the predefined maximum number of iterations is reached a further

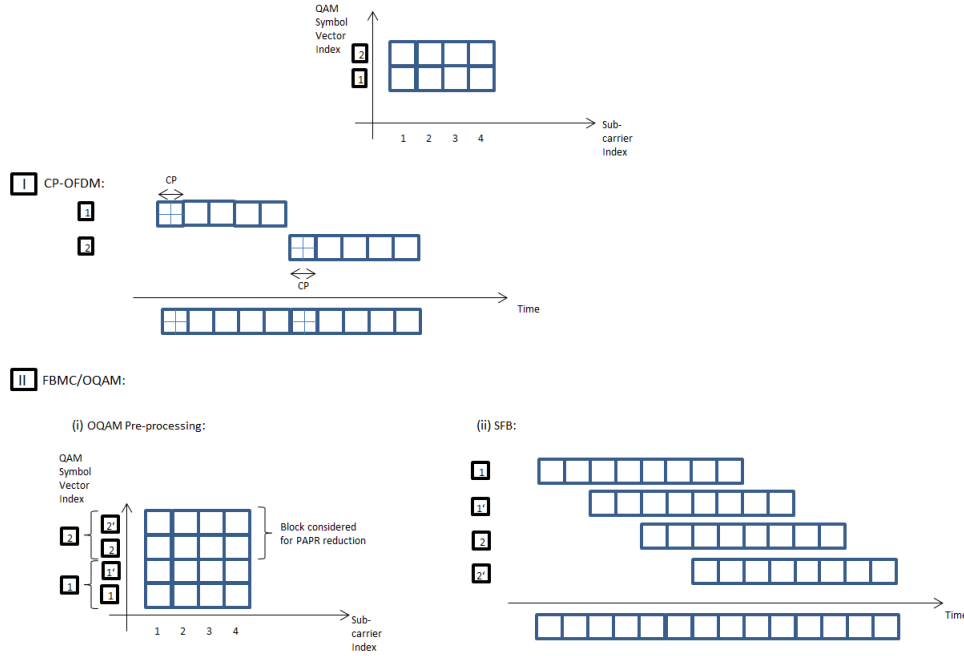


Fig. 2. FBMC/OQAM (left) vs. CP-OFDM (right) time signal.

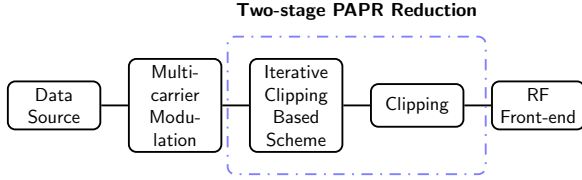


Fig. 3. Two-stage PAPR reduction scheme block diagram.

clipping is applied giving the final output. Figure 3 gives a simplified block diagram for the ‘two-stage PAPR reduction’.

Finally, SLM will be modified in order to benefit from the special structure of the FBMC/OQAM’s time signal, Figure 2, and is called ‘mSLM’. This scheme will be similar to the scheme proposed in [12] for wavelet OFDM, where it considers U^K hypotheses instead of just U as in the regular SLM. Offering a potential for improved PAPR reduction performance as a result, however at the expense of a rather great increase in computational complexity. The algorithm of mSLM scheme involves the following steps.

- 1) Several different candidate QAM symbol vectors $\mathbf{X}^u = [X_0^u, X_1^u, \dots, X_{M-1}^u]^T$ based on the same input QAM symbol vector $\mathbf{X} = [X_0, X_1, \dots, X_{M-1}]^T$ are generated through component wise multiplication of \mathbf{X} with the phase sequences $\mathbf{P}^u = [P_0^u, P_1^u, \dots, P_{M-1}^u]^T$; $u = 1, \dots, U$.
- 2) The components $P_m^u, m = 0, \dots, M-1$, of the phase sequence \mathbf{P}^u are unit magnitude complex numbers, where $P_m^u = \exp(j\varphi_m^u)$; $\varphi_m^u \in [0, 2\pi)$. Generally $P_m^u \in \{\pm 1\}$ or $P_m^u \in \{\pm 1, \pm j\}$ are often used.

- 3) The U different candidate QAM symbol vectors \mathbf{X}^u are then modulated using the respective FBMC/OQAM modulator, giving U different SLM signal vectors \mathbf{y}^u .
- 4) Until step (3) this is exactly as for the regular SLM. However, now for FBMC/OQAM the overlap between the symbols are to be taken into consideration by considering K overlapping QAM symbol vectors instead of considering each individually. This means that we now have U^K hypotheses:

$$\hat{s}^{(\mathbf{u})}[k] = \sum_{n'=-\infty}^{n-1} s_{n'}[k + (n - n')M] + \sum_{\nu=0}^{K-1} s_{n+\nu}^{(u_\nu)}[k - \nu M] \quad (2)$$

Where $\mathbf{u} \triangleq [u_\nu] = [u_0, u_1, \dots, u_{K-1}]$, with the first part of the equation denoting the signal that has been generated until step n .

- 5) Now a PAPR value is calculated for every $\hat{s}^{(\mathbf{u})}[k]$, from which the optimum \tilde{u} that gives the minimum PAPR is identified. Then finally $\hat{s}^{(\tilde{u}_0)}[k]$ is selected for transmission at step n .
- 6) In the next step $n + 1$, all the hypotheses with $u_0 = \tilde{u}_0$ can be reused, each left-shifted by M and filled with U candidates of the next FBMC/OQAM symbol $n + K$.

IV. RESULTS

In the final paper, the results obtained from simulating the various PAPR reduction schemes that were mentioned in Section III for both OFDM and FBMC/OQAM based systems are going to be presented. Firstly, by evaluating their PAPR

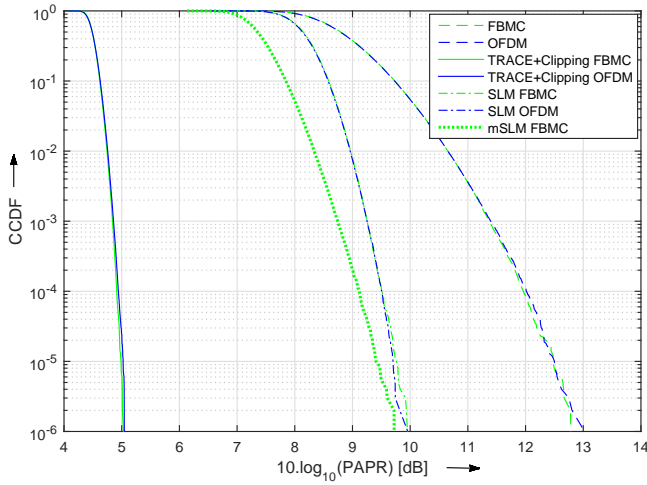


Fig. 4. CCDF of OFDM and FBMC/OQAM PAPR with and without PAPR reduction.

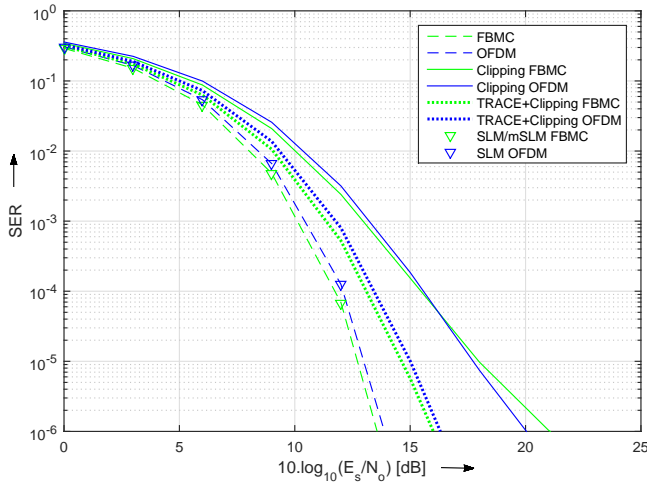


Fig. 5. SER of OFDM and FBMC/OQAM with and without PAPR reduction.

reduction performance with initial results shown in Figure 4. Then, by doing a performance evaluation in terms of SER with initial results shown in Figure 5. To ensure a fair comparison, both OFDM and FBMC/OQAM will have the same size of the time domain frame, total number of sub-carriers and number of data sub-carriers. Additionally, a fixed complexity for all PAPR reduction schemes is going to be set.

REFERENCES

- [1] M. Bellanger, D. Le Ruyet, D. Roviras, M. Terré, J. Nossek, L. Baltar, Q. Bai, D. Waldhauser, M. Renfors, T. Ihalainen *et al.*, "FBMC physical layer: a primer," *PHYDYAS*, January, 2010.
- [2] J. A. Bingham, "Multicarrier modulation for data transmission: An idea whose time has come," *IEEE Communications Magazine*, vol. 28, no. 5, pp. 5–14, 1990.
- [3] A. Viholainen, M. Bellanger, and M. Huchard, "Prototype filter and structure optimization," *website: www.ict-phydyas.org: Document D5.1*, 2009.
- [4] S. H. Han and J. H. Lee, "An overview of peak-to-average power ratio reduction techniques for multicarrier transmission," *IEEE Wireless Communications*, vol. 12, no. 2, pp. 56–65, 2005.
- [5] D.-W. Lim, S.-J. Heo, and J.-S. No, "An overview of peak-to-average power ratio reduction schemes for ofdm signals," *Journal of Communications and Networks*, vol. 11, no. 3, pp. 229–239, 2009.
- [6] Z. Kollár, L. Varga, and K. Czimer, "Clipping-based iterative papr-reduction techniques for fbmc," in *Proceedings of 17th International OFDM Workshop 2012 (InOWo'12)*, 2012, pp. 1–7.
- [7] M. Tanda, T. Fusco, M. Renfors, J. Louveaux, and M. Bellanger, "Data-aided synchronization and initialization (single antenna)," *website: www.ict-phydyas.org: Document D2.1*, 2008.
- [8] K. W. Martin, "Small side-lobe filter design for multitone data-communication applications," *IEEE Transactions on Circuits and Systems II: Analog and Digital Signal Processing*, vol. 45, no. 8, pp. 1155–1161, 1998.
- [9] A. Gatherer and M. Polley, "Controlling clipping probability in dmt transmission," in *IEEE Conference Record of the Thirty-First Asilomar Conference on Signals, Systems, and Computers*, 1997, vol. 1, 1997, pp. 578–584.
- [10] D. L. Jones, "Peak power reduction in ofdm and dmt via active channel modification," in *IEEE Conference Record of the Thirty-Third Asilomar Conference on Signals, Systems, and Computers*, 1999, vol. 2, 1999, pp. 1076–1079.
- [11] R. W. Bäuml, R. F. Fischer, and J. B. Huber, "Reducing the peak-to-average power ratio of multicarrier modulation by selected mapping," *Electronics Letters*, vol. 32, no. 22, pp. 2056–2057, 1996.
- [12] M. Hoch, S. Heinrichs, and J. B. Huber, "Peak-to-average power ratio and its reduction in wavelet-ofdm," in *International OFDM Workshop*, 2011, pp. 56–60.